Minireview

EVH1 domains: structure, function and interactions

Linda J. Ball[a,*], Thomas Jarchau[b], Hartmut Oschkinat[a], Ulrich Walter[b]

[a] *Forschungsinstitut für Molekulare Pharmakologie, Campus Berlin-Buch, Robert-Rössle Str. 10, 13125 Berlin, Germany*
[b] *Institut für Klinische Biochemie und Pathochemie, Versbacher Str. 5, D-97078 Würzburg, Germany*

Received 30 October 2001; revised 9 November 2001; accepted 3 December 2001

First published online 20 December 2001

Edited by Gianni Cesareni and Mario Gimona

Abstract ***Drosophila*** **enabled/vasodilator-stimulated phosphoprotein homology 1 (EVH1) domains are 115 residue protein–protein interaction modules which provide essential links for their host proteins to various signal transduction pathways. Many EVH1-containing proteins are associated closely with actin-based structures and are involved in re-organization of the actin cytoskeleton. EVH1 domains are also present in proteins enriched in neuronal tissue, thus implicating them as potential mediators of synaptic plasticity, linking them to memory formation and learning. Like Src homology 3, WW and GYF domains and profilin, EVH1 domains recognize and bind specific proline-rich sequences (*PRS*s). The binding is of low affinity, but tightly regulated by the high specificity encoded into residues in the protein:peptide interface. In general, a small (3–6 residue) 'core' *PRS* in the target protein binds a 'recognition pocket' on the domain surface. Further affinity- and specificity-increasing interactions are then formed between additional domain epitopes and peptide 'core-flanking' residues. The three-dimensional structures of EVH1:peptide complexes now reveal, in great detail, some of the most important features of these interactions and allow us to better understand the origins of specificity, ligand orientation and sequence degeneracy of target peptides, in low affinity signalling complexes.**

Key words: *Drosophila* enabled/vasodilator-stimulated phosphoprotein homology 1 domain; Actin cytoskeleton; Signal transduction; High resolution structure; Proline-rich sequence recognition; Class I and class II binding modes; Affinity/specificity control

1. Introduction

Drosophila enabled (Ena)/vasodilator-stimulated phosphoprotein (VASP) homology 1 (EVH1) domains [1,2] are found in a large number of multi-domain signalling proteins which are often involved in modulating the actin cytoskeleton or in signal transduction in postsynaptic compartments of certain chemical synapses. Proteins containing EVH1 domains include the Ena/VASP, Wiscott-Aldrich syndrome (WASP), RanBP1/nucleoporin and synaptic terminal protein (Homer, Vesl) families (Fig. 1). The Ena/VASP protein family, whose members are associated with adherens-type cell–matrix and cell–cell junctions, microfilaments and highly dynamic membrane regions [3], is perhaps the best studied of these families and comprises Ena, and its mammalian counterparts, Mena (mammalian Ena), VASP, and Evl (Ena/VASP-like protein). Mechanistically, Ena/VASP proteins are thought to enhance/accelerate actin filament formation by recruiting polymerization competent profilin–actin complexes to their proline-rich binding partners. Recruitment of profilin–actin is mediated by GPPPPP motifs present in the central, low complexity region of Ena/VASP proteins, whereas the highly conserved N-terminal EVH1 domain mediates specific binding to cytoskeleton-associated partners containing FPPPP motifs, such as zyxin [4], vinculin [5] and the listerial ActA protein [6], amongst others. An additional C-terminal Ena/VASP homology 2 (EVH2) domain is required for tetramerization/oligomerization and F-actin binding, which affects indirectly the EVH1-mediated interactions [1,7]. In contrast to the stimulatory roles of Ena/VASP proteins in actin-based listerial motility [8,9] and formation of membrane protrusions [10,11], increasing evidence is emerging which also suggests inhibitory roles of Ena/VASP proteins with respect to axon guidance [12,13], cyclic nucleotide-dependent inhibition of platelet integrin function [14,15] and inhibition of plasma membrane activity and random motility in fibroblasts [16].

The WASP family proteins are also closely associated with cytoskeleton regulation and are believed to regulate actin assembly downstream of Cdc42 and phosphatidylinositol 4,5-bisphosphate signalling pathways. Their N-terminal EVH1 domains (sometimes referred to as WH1 domains) bind proline-rich sequences (*PRS*s) in the WASP interacting protein, which is also involved in actin re-organization. The Homer-Vesl proteins show no obvious connection to the actin assembly machinery, but are found enriched in neuronal tissue. These proteins are proposed to play a role in long-term potentiation in excitatory synapses, with implications for memory formation [17]. Homer-Vesl EVH1 domains bind selectively to the C-termini of group I metabotropic glutamate receptors (mGluRs), inositol-1,4,5-trisphosphate receptors (IP3Rs), ryanodine receptors (RyRs) and the Shank family proteins [18–20].

The protein–protein interactions mediated by EVH1 domains are clearly highly important for the regulation of signal transduction events, re-organization of the actin cytoskeleton, and modulation of actin dynamics and actin-based motility. Here, we will review the structure, function and molecular binding characteristics of EVH1 domains in their known complexes.

*Corresponding author.
E-mail address: linda@fmp-berlin.de (L.J. Ball).

0014-5793/02/$22.00
PII: S0014-5793(01)03291-4

2. EVH1 domains as low affinity, protein–protein interaction modules

The EVH1 domains [1,2] comprise an important family of small, non-catalytic, protein interaction domains which specifically bind target proline-rich sequences (*PRS*s) [4–8]. Like the Src homology 3 domains [21,22], WW domains [23,24], GYF domains [25,26] and profilin proteins [27,28], EVH1 domains interact with their target *PRS*s with remarkably low affinity (K_d values typically between 1 and 500 μM), yet nevertheless high specificity [8,29]. The relevance of low affinity interactions in the regulation of signalling events, where large, multi-protein signalling complexes are required to form and dissociate in sensitive response to external stimuli, is immediately clear. However, more intriguing is how these interactions maintain, at the same time, such high specificities. In order to understand the mechanisms which allow these apparently conflicting functional properties to be satisfied, we need to draw clues from the high resolution structures of these domains in complex with their ligands. Combining this information with mutational studies and other biophysical methods, we can then go on to understand how small complementary epitopes in both ligand and domain are used in nature to modulate the affinities of these interactions, in order to fulfil biological requirements.

3. EVH1 classification according to consensus *PRS* motifs

EVH1 domains can be divided into two classes based on the consensus sequences of their target *PRS* ligands (Fig. 2). The Ena/VASP family of proteins comprise the first class and specifically recognize FPPPP-containing sequences [8]. Single residue peptide substitution experiments have shown the consensus binding motif for class I EVH1 domains to be FPxϕP (where ϕ is a hydrophobic residue) [29]. Such sequences are found in a number of mammalian proteins, including the focal adhesion proteins zyxin and vinculin, as well as in the ActA protein of the intracellular pathogen, *Listeria monocytogenes* [4,5,8]. The complete list to date is shown in Fig. 2 (for a recent review, see [30]). Class II EVH1 domains are found in the Homer-Vesl protein family of postsynaptic receptor-associated proteins [18,31]. These recognize a distinct consensus *PRS*, with a core motif comprising PPxxF, found in the group I mGluRs, IP3Rs, RyRs and the Shank family proteins [19,20] (Fig. 2). The experimentally derived consensus *PRS* motif recognized by class I EVH1 domains is shown in Fig. 3 (data shown are for the human VASP protein [29]). For both VASP and Mena EVH1 domains, we showed, by substituting in turn each amino acid in the peptide target sequence, that proline residues at positions (−1) and (2) (FPPPP) (numbering as in Figs. 3 and 5) were essential for EVH1 binding [29]. In contrast, the prolines at positions (0) and (1) (FPPPP) were highly variable. Position (0) was completely non-specific and could be replaced by almost any other residue, whereas position (1) required a hydrophobic residue, Pro, Leu, Ala, Ile, Val or Phe, in order to maintain detectable EVH1 binding.

It has long been known that in aqueous solution, sequences highly rich in proline spontaneously form an extended element of secondary structure termed the left-handed PPII helix ($\phi = -78°$, $\varphi = +146°$) shown in Fig. 3 [32,33] (for a review, see [34]). This structure is triangular in cross section, and generally contains proline residues in at least every third amino acid position, thereby providing a hydrophobic interface of pyrrolidine rings along one edge of the PPII prism. Although proline usually dominates the composition of PPII helices, it is not obligatory within this element of secondary structure. In sequences with more than three amino acids, Val, Gln, Ser, Arg, Ala, Thr, Asp, Glu show a high preference for PPII structures, generally in that order [33]. In longer sequences, the frequency of non-proline amino acids generally follows the order: Gln, Arg, Ala, Leu, Ser, Asp, His and Glu [33]. It is therefore no surprise that it is mostly these amino acids which directly flank or punctuate the proline stretches of the core *PRS* motifs. In its complex with class I EVH1 domains, the *PRS* motif FPPPP maintains almost perfectly the PPII helix structure, whereas in the class II complex of Homer-1a, the *PRS* ligand, TPPSPF, shows a somewhat distorted version of this structure [35]. The differences in the bound peptide geometries can be rationalized in terms of the specific interactions formed with the *PRS* binding sites of the two classes of EVH1 domains. This provides a mechanism for specific targeted recognition.

4. High resolution structures of EVH1 domains and the *PRS* recognition site

The high resolution, three-dimensional structures of five EVH1 domains from different host proteins are now known [29,35–38]. The overall fold consists of a compact parallel β-sandwich, closed along one edge by a long α-helix, highly homologous to the pleckstrin homology (PH) and phosphotyrosine binding (PTB) domains [39]. The Cα traces superimposed in Fig. 4 show clearly that these structures are all almost identical, with minor differences in some loop regions, where amino acid insertions or deletions occur. The highly conserved residues essential for hydrophobic core packing, and therefore crucial for the correct folding of the domains, are marked with blue bars in Fig. 1. The importance of some of these residues in stabilizing the fold of the domain has been

→

Fig. 1. Alignment of the EVH1 domain sequences most closely related to those whose three-dimensional structures have now been determined. Red: acidic; blue: basic; green: hydrophobic; yellow: aromatic; and purple: polar residues. Gly and Pro are shown in dark green and orange, respectively. Red arrows highlight residues comprising the exposed aromatic cluster, which bind *PRS* motifs. Blue bars mark the most highly conserved regions. GenBank accession codes from top to bottom are: BC005773 (homer3; mm/mouse), AB020879 (vesl3; rn/rat), AF093265 (homer3; hs/human), AF093262 (homer1b; hs/human), AF093257 (homer1a; mm/mouse), AF093258 (homer1b; mm/mouse), AB019479 (vesl1l; mm/mouse), U92079 (homer; rn/rat), AJ276327 (homer1a; rn/rat), AF093267 (homer1b; rn/rat), AF093268 (homer1c; rn/rat), AB003726 (vesl; rn/rat), AB007688 (vesl1l; rn/rat), AF093263 (homer2a; hs/human), AF093264 (homer2b; hs/human), AF093259 (homer2a; mm/mouse), AF093260 (homer2b; mm/mouse), AB007689 (vesl2; rn/rat), AF093266 (homer; dm/fly), Z46389 (vasp; hs/human), AF084548 (vasp; mm/mouse), Z46388 (vasp; cf/dog), AF112209 (evl; hs/human), U72519 (evl; mm/mouse), NM_024147 (evl; rn/rat), AB017437 (ena; av/chicken), U72520 (mena; mm/mouse), U21123 (ena; dm/fly), AY007501 (lena; hm/leech), AB063495 (spred1; mm/mouse), AB063496 (spred2; mm/mouse), JC5909 (ae33; dm/fly).

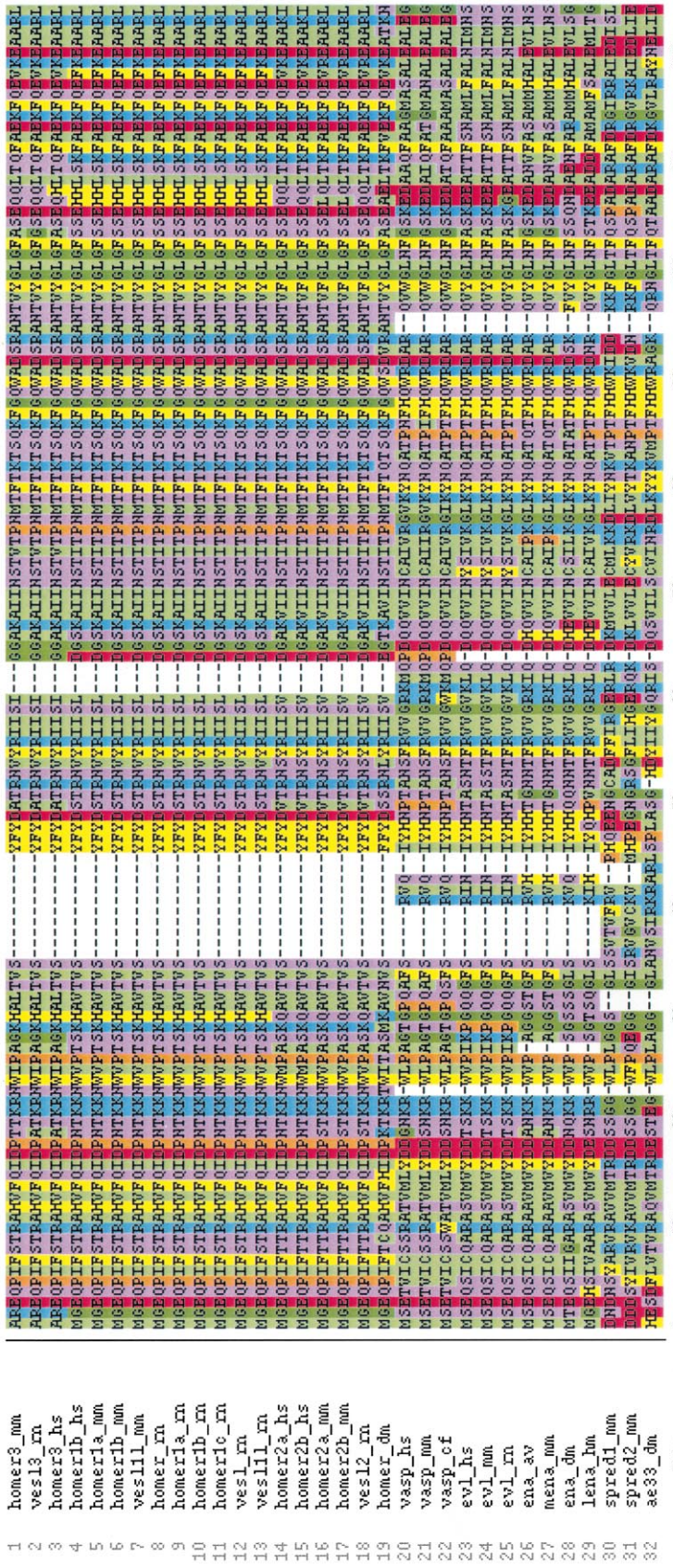
1 homer3_mm
2 vesl3_rn
3 homer3_hs
4 homer1b_hs
5 homer1a_mm
6 homer1b_mm
7 vesl1l_mm
8 homer_rn
9 homer1a_rn
10 homer1b_rn
11 homer1c_rn
12 vesl_rn
13 vesl1l_rn
14 homer2a_hs
15 homer2b_hs
16 homer2a_mm
17 homer2b_mm
18 vesl2_rn
19 homer_dm
20 vasp_hs
21 vasp_mm
22 vasp_cf
23 evl_hs
24 evl_mm
25 evl_rn
26 ena_av
27 mena_mm
28 ena_dm
29 lena_hm
30 spred1_mm
31 spred2_mm
32 ae33_dm
Ruler
1
10
20
30
40
50
60
70
80
90
100
110
120

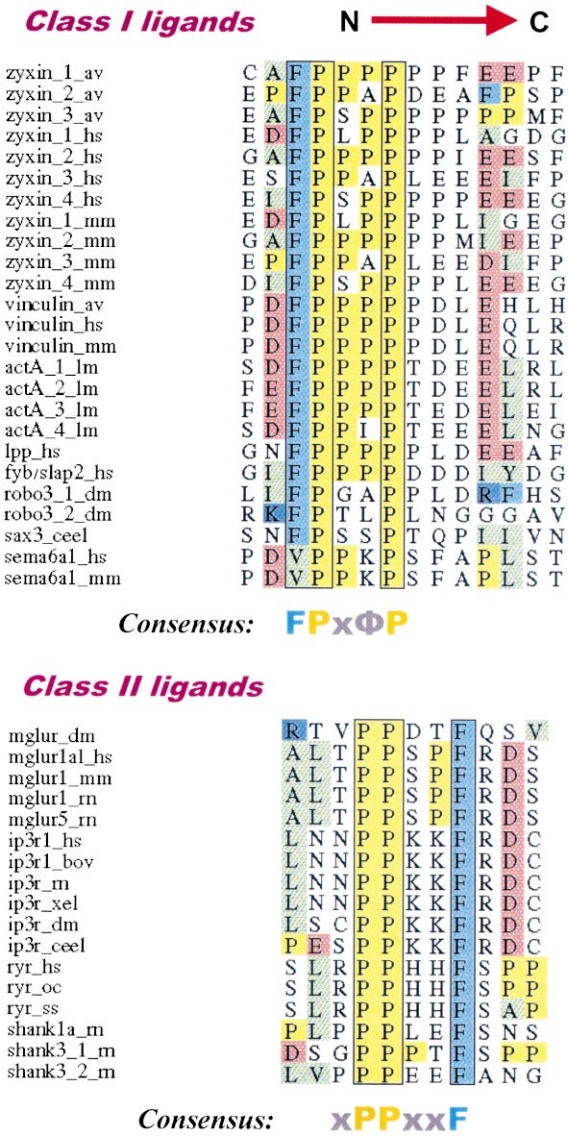

Fig. 2. Sequences of known class I and class II EVH1 target peptides, located in EVH1 binding partners. The class I peptides often occur in close tandem repeats as in zyxin and ActA. Consensus core residues are shown in yellow and cyan and conserved core-flanking epitopes are colored red (acidic), blue (basic) and green (hydrophobic). The GenBank accession codes of the EVH1 class I ligands from top to bottom are: X69190 (zyxin, repeats 1–3; av/chicken), X94991 (zyxin, repeats 1–4; hs/human), Y07711 (zyxin, repeats 1–4; mm/mouse), J04126 (vinculin; av/chicken), M33308 (vinculin; hs/human), L18880 (vinculin; mm/mouse), X59723 (ActA, repeats 1–4; lm/*L. monocytogenes*), NM_005578 (lpp, hs/human), AF198052 (fyb/slap2; hs/human), AF312580 (robo3, repeats 1–2; dm/fly), AF041053 (sax3; ceel/worm), AF279656 (sema6a1; hs/human), AF288666 (sema6a1; mm/mouse). For the class II ligands they are: X99675 (mGluR; dm/fly), U31215 (mGluR1α; hs/human), AF320126 (mGluR1; mm/mouse), NM_017011 (mGluR; rn/rat), D10891 (mGluR5; rn/rat), D26070 (IP3R1; hs/human), AF157625 (IP3R1; bov/cow), J05510 (IP3R; rn/rat), D14400 (IP3R; xel/frog), AJ238949 (IP3R; dm/fly), AF168688 (IP3R; ceel/worm), J05200 (RyR; hs/human), X15750 (RyR; oc/rabbit), M91452 (RyR; ss/pig), AF131951 (shank1a; rn/rat), AF133301 (shank3, repeats 1–2; rn/rat).

verified by mutational studies [40]. The backbone root mean square deviations (RMSDs) (calculated over all Cα, N, C′ atoms) of each EVH1 domain relative to every other are summarized in the table of Fig. 4. It is clear from these numbers that the largest structural variations occur between EVH1 domains of different classes.

In all EVH1 domains, a highly conserved cluster of three, surface-exposed aromatic sidechains (Tyr16, Trp23 and Phe79; VASP numbering) forms the recognition site for their target *PRS* ligands (Figs. 4 and 5). These positions are marked on the alignment in Fig. 1 as red arrows. Only in the Homer-Vesl EVH1 domains is one of these sidechains, Tyr16, replaced by an aliphatic residue, Ile16. Invariant to all EVH1 domains is the Trp residue at position 23 (Fig. 1), which is not only important for ligand docking, but also makes core hydrophobic contacts essential for correct folding. Mutation of this Trp residue to leucine (W23L) resulted in insoluble, inactive aggregates for which no binding constants could be measured [29]. This observation is in agreement with similar inactivating mutations analyzed in a yeast two-hybrid system [41]. The Trp23 sidechain is positioned between the Phe79 (conserved in class I and class II) and Tyr16 (the latter conserved in the class I EVH1 domains only), and together these form an exposed, hydrophobic 'sticky' platform with the correct geometry to dock the PPII- and PPII-based structures common to *PRS* ligands. The substitution of Tyr16 for Ile in the Homer-Vesl domains implies that some very different contacts are made in Homer-Vesl 'class II' interactions. The size and shape of the binding cleft between Trp23 and Ile16 are therefore modified, allowing a possible mechanism for selective binding of class II peptides (Figs. 2 and 5). Preliminary information like this already provides interesting clues as to the basis of specificity control by the different classes of EVH1 domains.

5. Structural rationalization of *PRS* specificity

To date, the structures of four EVH1 domains in complex with *PRS* ligands have been solved [29,35–37]. The surface-exposed, ligand recognition sites together with their *PRS* ligands are superimposed in Fig. 5. With this information in hand, it is possible to rationalize some of the experimental ligand binding data available. In both class I and class II EVH1 domains, the conserved Phe at position 79 forms a hydrophobic cleft between its own sidechain and that of Trp23, angled at approximately 90° to each other, into which the pyrrolidine ring of Pro(2) packs efficiently (Fig. 5). In class I domains, which bind FPxϕP, a second hydrophobic cleft of similar shape and size is created between the sidechains of Tyr16 and Trp23, into which the Pro(−1) ring packs. This hydrophobic cleft is absent in class II EVH1 domains due to the substitution of Tyr16 by Ile16. From inspection of the structure of the Homer-1a EVH1 complex with the class II peptide, TPPSPF (Fig. 5), it is clear that such a cleft would not be so useful here, as this ligand lacks a proline sidechain in the correct position to occupy it (i.e. position (−1) in the numbering of Fig. 5). Therefore ligand specificity in class II EVH1 domains must be encoded elsewhere, perhaps in the Phe at position (5) and in residues further removed from the core motif, such as the C-terminal Asp residue in the extended class II consensus sequence PPxxFxD [38]. Further structural studies using longer peptides will be needed before

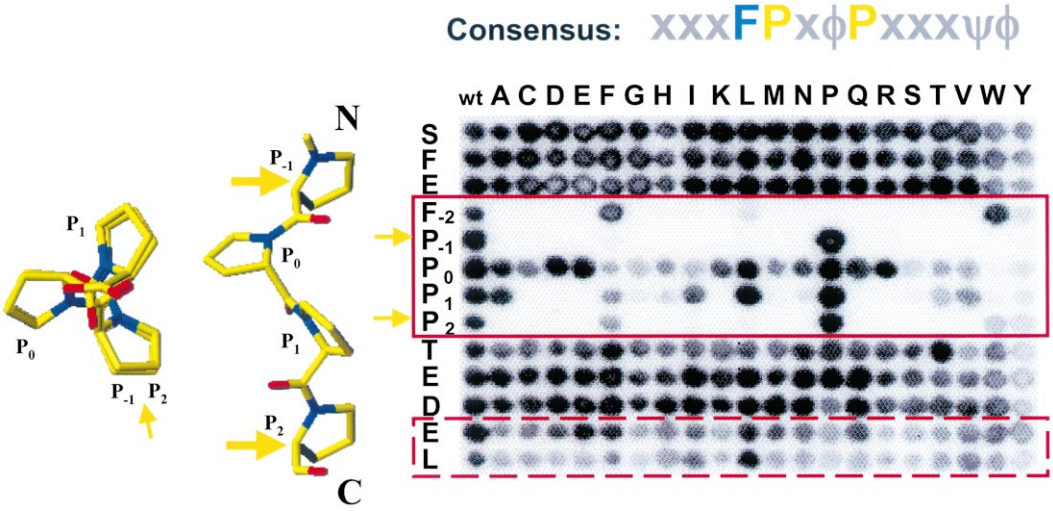

Fig. 3. Left: the PPII left-handed helix structure [32,33], showing the triangular cross section and the view along the length of the chain. It can be seen clearly that every third proline aligns along the same face, as illustrated here for Pro(−1) and Pro(2). Right: single residue substitution analysis of the EVH1 binding *PRS* peptide 'SFEFPPPPTEDEL' from the third ActA *PRS* repeat (ActA residues 332–344). Peptide residues were substituted in turn for all natural amino acid alternatives (rows) and assayed for binding to the VASP EVH1 domain [29]. The far left column is a control, showing the binding of the wild-type sequence. Spot intensities reflect the EVH1 binding affinities of each peptide measured. The FPPPP core sequence is enclosed by the red box and the C-terminal 'EL' epitope, responsible for increasing EVH1 binding affinity, is enclosed by a dashed red box. Yellow arrows mark the conserved prolines.

the origin of specificity in class II interactions can be fully understood.

The close packing interactions of Pro(−1) and Pro(2) of the peptide core motif (FPPPP) into the class I EVH1 surfaces explain their strict conservation in all Ena/VASP binding peptides (Figs. 2 and 3). The variability of the two central prolines in class I ligands can also be explained by the structures of the complexes: Pro(0) is oriented such that its sidechain makes no contact with the domain surface, thus allowing a wide variety of sidechains at this position; and Pro(1) makes very few contacts, resulting in only the more general requirement for a hydrophobic residue at position (1). In Homer complex with TPPSPF, the pattern of strictly conserved and unconserved peptide residues can be similarly rationalized. The Ser(3), Pro(4) residues induce a type VIa β-turn which modifies the PPII helix geometry so that the ligand twists away from the surface of the domain [35]. The sidechains of Ser(3) and Pro(4) are therefore, not surprisingly, divergent between the various ligands of the different Homer proteins. In class II interactions, Pro(−1) is replaced by a different sidechain, but in most cases, one of a hydrophobic nature which could then pack into the alternatively shaped hydrophobic cleft formed between Trp24 and Ile16 (Homer-1a numbering; see Fig. 5).

Another important feature of EVH1–*PRS* interactions is the conservation of a hydrogen bond between the indole NH of Trp23 and the carbonyl oxygen of the ligand Pro(0) (Fig. 5). A second, conserved hydrogen bond between Gln81 and the carbonyl oxygen of the peptide Pro(−1) is also seen in all of the class I EVH1 complexes, and based on the structural

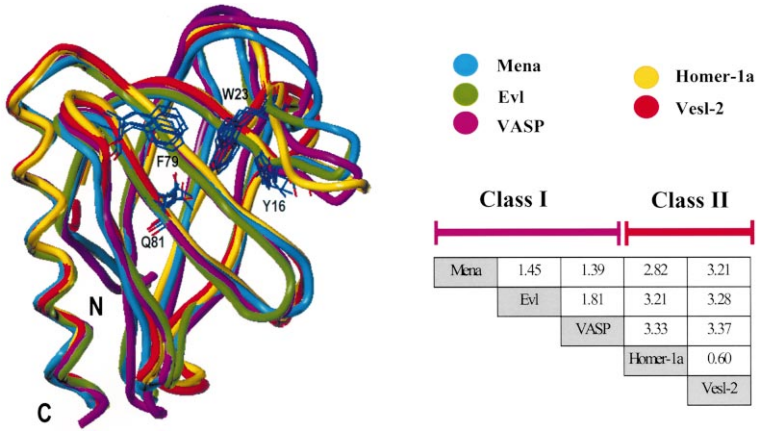

Fig. 4. Superposition of the backbone (N, Cα, and C′) atoms of the five EVH1 domains for which high resolution structures are now available: Mena (cyan), Evl (green), VASP (magenta), Homer-1a (yellow) and Vesl-2 (red) [29,35–38]. The residues of the aromatic triad, Tyr16, Trp23, Phe79 (VASP numbering), are shown in blue. Backbone (Cα, C′, N) RMSDs (Å) of each EVH1 structure relative to all others are summarized in the table. The classification into class I and class II domains is also given.

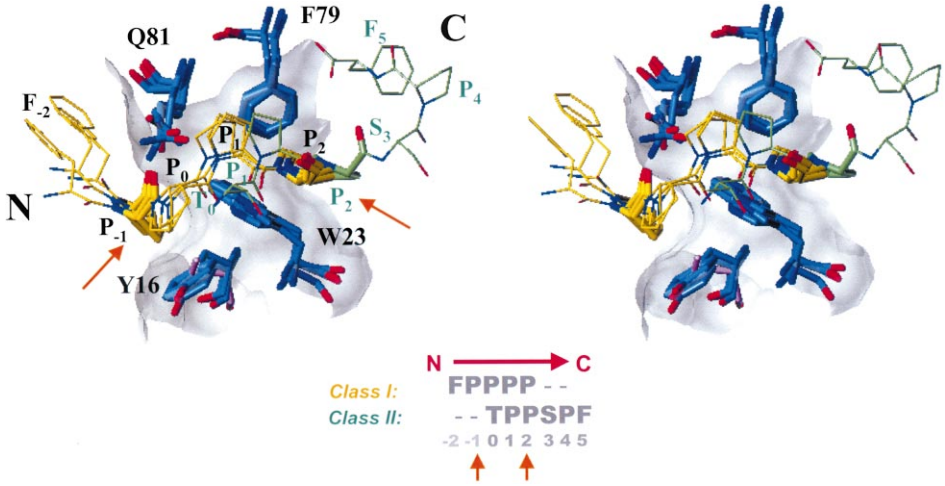

Fig. 5. Superposition (shown in stereoview) of the exposed, *PRS*–ligand recognition sites from the structures of the four known EVH1–*PRS* complexes (Mena, Evl, VASP and Homer-1a) [29,35–37]. The most important sidechains involved in the protein–ligand interaction are rendered in bold. The Ena/VASP (class I) peptides are shown in yellow and the Homer (class II) peptide is shown, and numbered, in green. It is clear that Pro(2) plays a crucial role in both classes of EVH1 interaction and that Pro(−1) is extremely important in the Ena/VASP class I interactions. In class I interactions, both Pro(−1) and Pro(2) sidechains pack very efficiently into the hydrophobic clefts created by the exposed Tyr, Trp, Phe triads on surfaces of class I EVH1 domains. In class II interactions, Pro(−1) is replaced by a different sidechain, but usually of a hydrophobic nature, which could then pack into the differently shaped hydrophobic pocket formed in class II EVH1 surfaces where Tyr16 is replaced by Ile16 (colored in pink). Also shown is the conserved position of Gln81, which contributes to peptide binding via hydrogen bond formation [29]. Numbering of the *PRS* ligands is based on defining position (0) as the first position common to both ligands in these complexes.

information examined so far, it is tempting to predict that this interaction should also be present in class II interactions. However, this hydrogen bond was not detected in the Homer complex and the peptide ligand studied in this case would need to be extended by at least one additional N-terminal amino acid to test this hypothesis. That both of these hydrogen bonds play important roles in ligand docking can be seen not only from their degree of conservation, but also experimentally, from the very large perturbations in both ^{15}N and ^{1}H chemical shifts of the donor Trp23 NH and Gln81 NH_2 atoms observed in nuclear magnetic resonance measurements carried out on the VASP EVH1 domain [29].

6. Ligand orientation, specificity and affinity regulation: the role of core-flanking residues

Flanking the core *PRS* motifs of all EVH1 ligands are residues or groups of residues comprising epitopes which modify interaction affinities, and as a result modulate specificity. Some of these residues are positioned directly next to the proline-rich region and constitute part of the actual consensus recognition motif, whereas other epitopes are several amino acids removed from the core. It is the interactions with the former class of epitopes which largely determine the binding orientation for otherwise highly symmetrical *PRS* peptide ligands. For example, the Ena/VASP EVH1 domains target very specifically, *PRS*s directly preceded by a single Phe residue (at the ligand (−2) position), which gives the ligand an unambiguous directionality. Phe(−2) is responsible for setting the register of binding in this class of EVH1 domains, ensuring that only Pro(−1) and Pro(2), and not the other prolines in the peptide, dock into the available clefts. Mutation of Phe(−2) to any amino acid, with the exception of Trp, results in loss of binding to EVH1 [8,29]. From the three known class I complex structures, we can see that the sidechain of Phe(−2) packs neatly into the peptide binding groove of the EVH1 domain [29,36,37]. However, docking experiments using molecular dynamics simulations have also suggested a possibility that FPPPP-containing ligands could bind in the opposite orientation, with Phe(−2) packing, albeit less efficiently, into an alternative hydrophobic site at the opposite end of this groove (Ball et al., unpublished results). There is therefore some scope for the possibility of forward and reverse binding modes in EVH1 domains. In Fig. 3, one can see that weak EVH1 binding occurs when a Phe (or Trp) residue replaces Pro(2). This could suggest that a small fraction of the peptide binds in the opposite orientation. However, if this was the case, one would also expect to see a corresponding faint spot in the column where Pro replaces Phe(−2), and no such spot is visible. It therefore seems more likely that the EVH1 domain is binding the mutant sequence, FPPPF (or FPPPW), than binding the FPPPP sequence in reverse. It might also be expected from the apparently reversed sequence of the Homer-1a target *PRS*, TPPSPF, that class II EVH1 domains should bind their peptides in the opposite orientation to the class I domains. Somewhat surprisingly, however, this is not the case and the TPPSPF peptide of Homer was shown to bind the Homer EVH1 domain with the same orientation as the Ena/VASP EVH1 domains [35]. Thus, although molecular dynamics simulations show that reverse polarity binding of EVH1 peptides is not sterically forbidden, there is to date no example of this. Interestingly, the class II peptide of the Human RyR differs from other class II peptides in its distribution of core-flanking basic and hydrophobic residues, which may have implications for reverse polarity binding. Whether EVH1 domains do indeed possess dual polarity peptide binding modes, however, remains to be confirmed experimentally.

Although orientation and specificity are partly controlled by the core motif, the binding affinities of isolated, short core peptides to EVH1 domains range from very weak to

undetectable. Further interactions are therefore needed to increase the affinities to appropriate levels. The modulation of binding affinity is largely under the control of epitopes a few amino acids further removed from the *PRS* core motif itself. These form either hydrophobic, hydrogen-bonded or electrostatic interactions with the domain surface. The hydrophobic surfaces of the EVH1 domains contain several small, additional hydrophobic patches close to the PPII binding groove [29]. One example is the area consisting of residues Gln31 to Phe33 in the Ena/VASP family (VASP numbering), which interacts with a conserved, affinity-raising EL epitope found C-terminal to each of the four FPPPP repeats in listerial ActA [29]. Because this epitope is absent in the endogenous Ena/VASP EVH1 binding partners, such as zyxin and vinculin (see Fig. 2), it is thought that the pathogen exploits the smaller, second hydrophobic EVH1 surface in order to increase its own binding affinity for EVH1 over that of the competing, native, zyxin/vinculin FPPPP-containing ligands [29]. In this way the ActA protein enables *Listeria* to successfully recruit EVH1-containing proteins for the synthesis of actin comet tails which provide the pathogen with the intracellular motility required for infection of neighboring cells. It has also been shown that acidic to basic mutations in the flanking residues of the second ActA FPPPP repeat severely reduce binding to the VASP EVH1 domain. However, binding was shown to be partially rescued ($\sim$3% binding regained) by complementary charge mutations on the EVH1 domain surface [41].

7. Conclusions

Combining structural information with biochemical methods, we can see that relatively minor structural variations on the EVH1 domain surfaces, together with corresponding complementary variations in their ligands can provide mechanisms for selectivity in *PRS* recognition. Importantly, such mechanisms do not exclude the possibility of overlapping peptide recognition, so that class I domains may well be able to bind to class II ligands and vice versa, albeit with reduced affinities. This allows the possibility for one EVH1-containing protein to rescue, at least to some extent, the effects of knocking out another, as observed experimentally [16,30,40,42]. This, in some cases, may prove highly valuable to the host cell. The available data suggest that EVH1 domains evolved from the versatile PH/PTB folding scaffold, and then diverged to fulfil specialized and partially overlapping functions in different cellular contexts, whilst maintaining the common ability to bind *PRS*s.

The high resolution structural information now available clarifies our understanding of the most important features of EVH1-mediated interactions and of the subtle factors which govern target specificity and binding affinity. This information can be used to facilitate the design of novel peptide, non-peptide and small organic molecule inhibitors which interfere with the binding of EVH1-containing proteins to their respective partners. Such rationally designed inhibitors would be useful in several ways. Firstly, and perhaps most importantly, highly selective EVH1 inhibitors would provide invaluable tools for the dissection of biochemical pathways, which could be used in a dose-dependent manner, to directly complement data from corresponding genetic knockout models. Secondly, appropriately modified EVH1 ligands would also find uses as molecular tags to monitor the formation and dissociation of EVH1-mediated interactions within the cell. And thirdly, such inhibitors may ultimately provide the precursors/lead molecules needed for the development of future generations of novel therapeutics, which could help in the treatment of diseases in which controlled or partial inhibition of EVH1-mediated events would be desirable (for example, the spreading of intracellular pathogens, pathologically altered adhesion and motility in inflammatory and metastatic diseases). All of these possibilities provide a great number of fascinating and challenging tasks for the future.

References

[1] Haffner, C., Jarchau, T., Reinhard, M., Hoppe, J., Lohmann, S.M. and Walter, U. (1995) EMBO J. 14, 19–27.
[2] Gertler, F.B., Niebuhr, K., Reinhard, M., Wehland, J. and Soriano, P. (1996) Cell 87, 227–239.
[3] Reinhard, M., Halbrugge, M., Scheer, U., Wiegand, C., Jockusch, B.M. and Walter, U. (1992) EMBO J. 11, 2063–2070.
[4] Reinhard, M., Jouvenal, K., Tripier, D. and Walter, U. (1995) Proc. Natl. Acad. Sci. USA 92, 7956–7960.
[5] Reinhard, M., Rüdiger, M., Jockusch, B.M. and Walter, U. (1996) FEBS Lett. 399, 103–107.
[6] Chakraborty, T. et al. (1995) EMBO J. 14, 1314–1321.
[7] Bachmann, C., Fischer, L., Walter, U. and Reinhard, M. (1999) J. Biol. Chem. 274, 23549–23557.
[8] Niebuhr, K. et al. (1997) EMBO J. 16, 5433–5444.
[9] Loisel, T.P., Boujemaa, R., Pantaloni, D. and Carlier, M.F. (1999) Nature 401, 613–616.
[10] Rottner, K., Behrendt, B., Small, J.V. and Wehland, J. (1999) Nat. Cell Biol. 1, 321–322.
[11] Castellano, F., Clainche, C.L., Patin, D., Carlier, M.F. and Chavrier, P. (2001) EMBO J. 20, 5603–5614.
[12] Bashaw, G.J., Kidd, T., Murray, D., Pawson, T. and Goodman, C.S. (2000) Cell 101, 703–715.
[13] Dickson, B.J. (2001) Curr. Opin. Neurobiol. 11, 103–110.
[14] Aszodi, A. et al. (1999) EMBO J. 18, 37–48.
[15] Hauser, W. et al. (1999) Proc. Natl. Acad. Sci. USA 96, 8120–8125.
[16] Bear, J.E., Loureiro, J.J., Libova, I., Fässler, R., Wehland, J. and Gertler, F.B. (2000) Cell 101, 717–728.
[17] Kato, A., Ozawa, F., Saitoh, Y., Hirai, K. and Inokuchi, K. (1997) FEBS Lett. 412, 183–189.
[18] Brakeman, P.R., Lanahan, A.A., O'Brien, R., Roche, K., Barnes, C.A., Huganir, R.L. and Worley, P.F. (1997) Nature 386, 284–288.
[19] Tu, J.C., Xiao, B., Yuan, J.P., Lanahan, A.A., Leoffert, K., Li, M., Linden, D.J. and Worley, P.F. (1998) Neuron 21, 717–726.
[20] Naisbitt, S. et al. (1999) Neuron 23, 569–582.
[21] Yu, H., Chen, J.K., Feng, S., Dalgarno, D.C., Brauer, A.W. and Schreiber, S.L. (1994) Cell 76, 933–945.
[22] Sparks, A.B., Rider, J.E., Hoffman, N.G., Fowlkes, D.M., Quillam, L.A. and Kay, B.K. (1996) Proc. Natl. Acad. Sci. USA 93, 1540–1544.
[23] Chen, H.I. and Sudol, M. (1995) Proc. Natl. Acad. Sci. USA 92, 7819–7823.
[24] Macias, M.J., Hyvonen, M., Baraldi, E., Schultz, J., Sudol, M., Saraste, M. and Oschkinat, H. (1996) Nature 382, 646–649.
[25] Nishizawa, K., Freund, C., Li, J., Wagner, G. and Reinherz, E.L. (1998) Proc. Natl. Acad. Sci. USA 95, 14897–14902.
[26] Freund, C., Dotsch, V., Nishizawa, K., Reinherz, E.L. and Wagner, G. (1999) Nat. Struct. Biol. 6, 656–660.
[27] Schutt, C.E., Myslik, J.C., Rozycki, M.D., Goonesekere, N.C. and Lindberg, U. (1993) Nature 365, 810–816.
[28] Mahoney, N.M., Janmey, P.A. and Almo, S.C. (1997) Nat. Struct. Biol. 4, 953–960.
[29] Ball, L.J. et al. (2000) EMBO J. 19, 4903–4914.
[30] Reinhard, M., Jarchau, T. and Walter, U. (2001) Trends Biochem. Sci. 26, 243–249.
[31] Kato, A., Ozawa, F., Saitoh, Y., Fukazawa, Y., Sugiyama, H. and Inokuchi, K. (1998) J. Biol. Chem. 273, 23969–23975.
[32] Cowan, P.M. and McGavin, S. (1955) Nature 176, 501–503.

[33] Adzhubei, A.A. and Sternberg, M.J. (1993) J. Mol. Biol. 229, 472–493.
[34] Williamson, M.P. (1994) Biochem. J. 297, 249–260.
[35] Beneken, J., Tu, J.C., Xiao, B., Nuriya, M., Yuan, J.P., Worley, P.F. and Leahy, D.J. (2000) Neuron 26, 143–154.
[36] Prehoda, K.E., Lee, D.J. and Lim, W.A. (1999) Cell 97, 471–480.
[37] Fedorov, A.A., Fedorov, E., Gertler, F. and Almo, S.C. (1999) Nat. Struct. Biol. 6, 661–665.
[38] Barzik, M., Carl, U.D., Schubert, W.D., Frank, R., Wehland, J. and Heinz, D.W. (2001) J. Mol. Biol. 309, 155–169.
[39] Saraste, M. and Hyvonen, M. (1995) Curr. Opin. Struct. Biol. 5, 403–408.
[40] Ahern-Djamali, S.M. et al. (1998) Mol. Biol. Cell 9, 2157–2171.
[41] Carl, U.D., Pollmann, M., Orr, E., Gertler, F.B., Chakraborty, T. and Wehland, J. (1999) Curr. Biol. 9, 715–718.
[42] Bear, J.E., Krause, M. and Gertler, F.B. (2001) Curr. Opin. Cell Biol. 13, 158–166.